Better Designing and Evaluation of Insulating Foamed Ceramics

V. R. Salvini, D. Spinelli, V. C. Pandolfelli

Given the importance of energy costs and environmental concerns, insulating foamed ceramics have received much attention in recent years. This group of porous materials presents key properties such as low density and thermal conductivity, controlled permeability and high surface area allowing their use in many industrial processes aiming to reduce heat losses and energy consumption.
However, they are subjected to stresses when used in use. Therefore, the understanding of the thermo-mechanical behaviour of these materials is a key issue for selection and design for structural applications. This paper is organized into two parts. The first one shows the effect of direct-foaming processing on the physical and morphological properties of macro-porous ceramics. The second part discusses the values of mechanical properties such as the compressive and flexural strengths, and the elastic modulus. In addition, a data compilation highlighting the relationship between porosity (P) and mechanical properties of foamed ceramics is shown. Finally, the results for the fracture toughness and the fracture energy of foamed ceramics are discussed. The paper also highlights that the understanding of the processing techniques and evaluation methods of porous ceramics are the correct path to generate suitable materials for a more sustainable environment where saving energy is a key aspect.

1 Introduction

Recently there has been wide interest in porous ceramics as a consequence of their properties, which comprise high porosity (up to 90 vol.-%), with open and interconnected or closed and isolated pores, and a broad range of sizes (micropores: d <2 nm; mesopores: 50 nm > d > 2 nm; macropores: d >50 nm). These features are useful for applications such as filters for liquid metals, supports for catalysis, bioceramics for bone regeneration and thermal insulating ceramics.
It is generally well-known that suitable properties for porous ceramics are close related to the fabrication process, which basically includes four categories: (1) partial sintering, (2) sacrificial fugitives, (3) replica templates and (4) direct foaming. Novel fabrication processes, their respective porous structure, processing factors and environmental issues have recently been reviewed by Ohji [1] and Salvini [2].
Despite the importance of this class of ceramic materials, there is not a general consensus regarding the dependence of mechanical properties on the porosity parameters. In other words, the actual data of these materials indicate that their mechanical behaviour depends on more than just their porosity.
Questions have been raised regarding the models proposed by Ashby et al. [3, 4], which indicate that the relative strength of a porous material is a function of its relative density as follows:

$$\frac{\sigma}{\sigma_s} = C \left(\frac{\rho}{\rho_s}\right)^m \quad (1)$$

where σ and ρ are, respectively, the fracture strength and the density of porous material; σ_s and ρ_s are the fracture strength and the density of solid material; C is a dimensionless constant and the exponent m depends on the pore morphology (m = 3/2 for open pores or m = 2 for closed ones).
Colombo et al. [5] have attributed the lack of fitting to the Ashby's models to some microstructural factors. According to that paper, Ashby's models do not consider the distribution of pores sizes, the presence of mixed closed and open pores or defects at the pore walls (struts).

Vânia R. Salvini, Dirceu Spinelli
University of São Paulo, EESC-USP
São Carlos, SP, 13565-905
Brazil

Victor C. Pandolfelli
Federal University of São Carlos, Materials Engineering Department
Materials Microstructure Engineering Group (GEMM), (FIRE Associate Laboratory)
São Carlos, SP, 13565-905
Brazil

Corresponding authors: *V. R. Salvini, V. C. Pandolfelli*
E-mail: pvrs@ufscar.br (V. R. Salvini) or vicpando@ufscar.br (V. C. Pandolfelli)

Keywords: foamed ceramics, environmental friendly processing, thermal insulating ceramics, mechanical properties

Received: 05.02.2015
Accepted: 12.02.2015
The paper was awarded with the 2nd prize at ALAFAR 2014

Rice [6] has already drawn attention to this debate presenting some concerns with micro-mechanics based models, as they assume that the application of a hydrostatic pressure is uniformly distributed in all pores. Zheng et al. [7] have considered that the fracture strength of brittle porous material is nonlinear and, therefore, there is a percolation failure phenomenon at the fracture of these materials. Based on that, this later model considers the porosity (P) and the elastic percolation (ϕ), which depends on the Poisson's ratio of material, as shown:

$$\frac{\sigma}{\sigma_S} = \left[\left(\frac{\phi - P}{\phi}\right)^{1+\nu} \cdot \left(1 - \phi^{2/3}\right)\right]^{1/2} \quad (2)$$

$$\phi = 1 - \left[\frac{1+\upsilon}{3(1-\upsilon)}\right] = \frac{2(1-2\upsilon)}{3(1-\upsilon)} \quad (3)$$

where, ν is the scaling exponent for tridimensional solids and υ is the Poisson ratio of materials. In general, for ceramics $\upsilon = 0{,}2$ and $\phi = 0{,}5$.

The authors of present work believe that meeting the challenge of correctly addressing porosity-mechanical property relations requires simplification of the problem, but in a way that does not distort the physical meaning.

In this context, the present work firstly point out the effect of the green direct-foaming processing on the physical and morphological properties of macro-porous ceramics of different compositions.

Then, the experimental data of mechanical strength, elastic modulus, fracture toughness and fracture energy are compared with the theoretical models in the literature for porous brittle materials. In this analysis the ceramic processing parameters are considered aiming for a better understanding about the mechanical behaviour of porous ceramics.

2 Materials and techniques

2.1 Materials

The green direct-foaming method developed by the authors [2] was applied to produce of the macro-porous Alumina (Al_2O_3), Alumina-Mullite ($3Al_2O_3 \cdot 2SiO_2$) and Silica (SiO_2) ceramics. The description and details of the developed direct-foaming processing are described in Salvini et al. [2].

Tab. 1 presents the ceramic compositions that were prepared based on calcined aluminas CL 370 and CT 3000SG (Almatis/DE), mullite Mulcoa #325 (Raw Kyanite/US), fused silicas Teco Sil and Teco Sil Fine (CE Minerals/US) and high alumina cement Secar 71 (Kerneos/FR) as the hydraulic inorganic binder.

Tab. 1 Foamed ceramic compositions

Raw Material	Composition [%]		
	Al_2O_3	Al_2O_3-Mullite	SiO_2
CL 370 + CT 3000SG	94,24	69,40	–
Mulcoa #325	–	24,78	–
Teco Sil + Teco Sil Fine	–	–	93,47
Secar 71	5,76	5,82	6,53

The chosen additives consisted of Castament FS60 (BASF) as dispersant, Rheocell-Rheofill (BASF) as foaming surfactant and the Methocell 306 (Dow Chemical) as thickening additive. All of them are non-toxic and make it feasible to produce high volume and stable aqueous based foams. All ceramic suspensions contained 53 vol.-% of solids.

2.2 Techniques

The foamed ceramic suspensions were cast into 25 mm × 25 mm × 150 mm bars and 40 mm × 40 mm cylindrical moulds. All samples were cured at 50 °C in a climatic chamber (Model VC 2020, Vötsch) under controlled humidity of ~80 % for 24 h. After that, the samples were demoulded and further dried in an oven for 24 h at 110 °C in air. Finally, they were sintered at 1500 °C for 5 h.

The density and porosity of the sintered samples were measured using the Archimedes method with kerosene as the fluid.

The flexural strength (σ_f) was conducted at room temperature in a three-point bending over a span of 125 mm and a crosshead speed of 1,3 mm/min (ASTM C133-97). The uniaxial compressive strength (σ_c) was also conducted at room temperature using the same crosshead speed (ASTM C133-97).

Although many researchers use a single test sample, in this research the work of fracture and notched beam tests were carried out on separate samples for the two fracture energy measurements, γ_{NBT} and γ_{WOF}. The γ_{NBT} represents the fracture surface energy to initiate crack propagation, whereas the work-of-fracture γ_{WOF} expresses the energy to propagate a crack through the specimen thickness [8, 9].

The critical stress intensity factor (K_{IC}), using the single edge notched beam technique (ASTM E-399), was determined at room temperature in a three-point bend test applying the equation:

$$K_{IC} = \frac{P \times S}{B \times W^{3/2}} \times f\left(\frac{a}{W}\right) \quad (4)$$

where P is the fracture load, S is the span, B is the specimen width, W is the specimen thickness, a corresponds to the crack size, and f (a/W) is obtained by the following expression:

$$f\left(\frac{a}{W}\right) = 3\sqrt{\frac{a}{W}} \times \frac{1.99 - \left(\frac{a}{W}\right) \times \left(1 - \frac{a}{W}\right)\left[2.15 - 3.93\frac{a}{W} + 2.7\left(\frac{a}{W}\right)^2\right]}{2\left(1 + 2\frac{a}{W}\right)\left(1 - \frac{a}{W}\right)^{3/2}} \quad (5)$$

For the K_{IC} measurements the bar samples were center-notched to one-half of their thickness (a/W ≈ 0,5) with a 300 µm thick diamond blade. All fracture energy tests were performed on MTS 180 machine in three-point bending over a span of 125 mm. For K_{IC}, the fracture surface energy (γ_{NBT}) measurements were carried out at stress loading rate of 1,5 kN/s.

The K_{IC} value was used to calculate the energy for crack initiation γ_{NBT} by the following expression:

$$K_{IC} = (2\,\gamma_{NBT}\,E)^{1/2} \quad (6)$$

where, E is Young's elastic modulus measured by a flexural resonance technique in bar samples. Further details about this procedure can be found in Pickett's paper [10].

For the γ_{WOF} measurements, the bar samples were also center-notched with a 300 µm thick diamond blade so that one-half of their thickness cross section remained. The γ_{WOF} samples were loaded in 3-point bend-

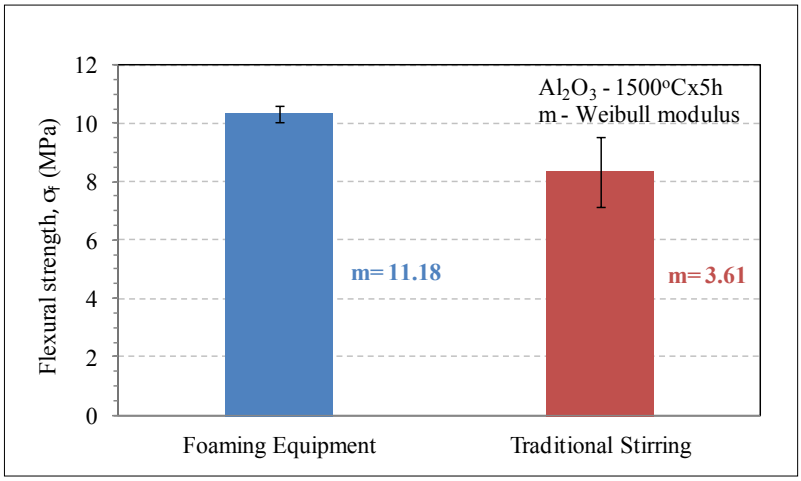

Fig. 1 **Flexural mechanical strength of foamed alumina produced by the traditional stirring method and by the foaming equipment**

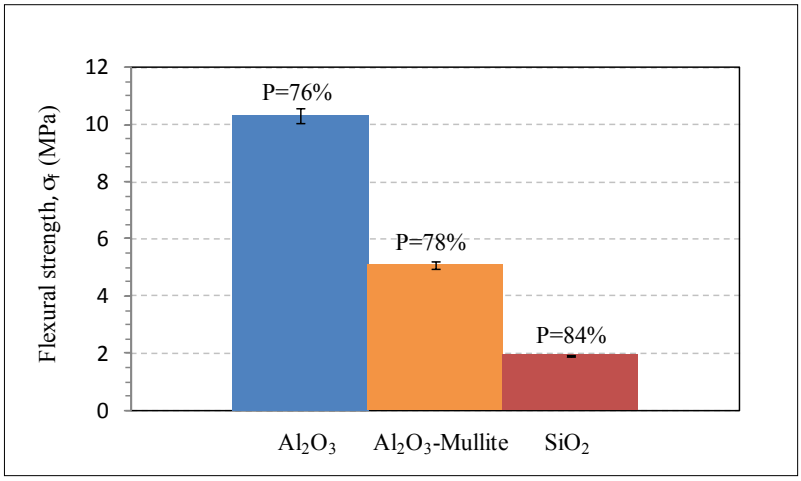

Fig. 2 **Flexural mechanical strength and porosity (P) of foamed ceramic compositions produced by the foaming equipment after sintering at 1500 °C for 5 h**

ing at a crosshead speed of 0,001 mm/min to ensure stable crack growth (ASTM C1368-10). The γ_{WOF} values were then calculated by:

$$\gamma_{WOF} = \frac{\int F\,dx}{2A} \qquad (6)$$

where, $\int F\,dx$ represents the required work for new surfaces generation and A is the projected area of the fracture surfaces directly measured by the individual specimen notched areas. Finally, the morphology and fracture surface of the macro-porous samples were investigated using scanning electron microscopy (Inspect S50).

3 Results and discussion

This section has been organized into two parts. The first one shows the effect of direct-foaming processing on the physical and morphological properties of macro-porous ceramics. The second part discusses the values of mechanical properties such as the compressive and flexural strengths, and the elastic modulus. In addition, a data compilation highlighting the relationship between porosity (P) and mechanical properties of foamed ceramics is shown. Finally, the results for the fracture toughness and the fracture energy of foamed ceramics are discussed.

3.1 Effect of foaming process on the physical and morphological properties

Fig. 1 depicts the flexural strength and the Weibull modulus (m) for the sintered macro-porous alumina samples produced by the foaming equipment and the traditional stirring method. For dense ceramics m values usually ranges from 5 to 13 [10]. It can be seen that both properties (σ_f and m) increase when the foaming equipment was used. The high values of m obtained for the foaming equipment agree with those by the Magrabi et al. [10], who found that Weibull-type distribution best describes the narrow bubble-size range resulted by a compressed-air foam generator.

Nevertheless, the mechanical strength of the foamed ceramics also depends on the density of the pore walls and struts, which can be improved by better packing the solid particles.

Fig. 2 presents the flexural strength and porosity level of the sintered foamed ceramics, all produced by the foaming equipment. It is clearly shown that the foamed compositions present distinct levels of mechanical strength and porosity, even using ceramic suspensions with the same concentration of solids (53 vol.-%). These differences in properties can be understood considering the concepts of solid particle packing and the mineralogical phases formed.

In order to maximize the packing of solids for the Al_2O_3 composition, the different particle size of raw materials used were adjusted by the PSDesigner software using the Andreasen packing model with q = 0,37.

However, in case of Al_2O_3-Mullite composition there was a deficiency of fines, increasing the difference between the theoretical model and the actual packing curves. Regarding the foamed SiO_2 composition, the main reason of low mechanical strength and high porosity level is due to the crystallization of the amorphous SiO_2 at sintering, forming the cristobalite phase, which shows high dimensional change on cooling leading to crack formation.

3.2 Mechanical properties

Alumina (Al_2O_3) ceramics with high porosity (76 %) and low thermal conductivity (<1 W/m · K) at 1200 °C were produced using the foaming method developed by the authors [2]. Tab. 2 presents a summary of the mechanical properties at room temperature for the foamed Al_2O_3 composition.

Fig. 3 shows the flexural and compression relative strength individual values attained as a function of relative density for foamed Al_2O_3, which are compared to the open-cell and closed-cell models proposed by Ashby and Gibson [3, 4].

Ashby's model considers two distinct morphologies of cell foams: 1) the open-cell foams containing interconnected struts and no cell walls, and 2) the closed-cell foams consisted of isolated cells with dense walls. Conversely, the morphology of foamed ceramics considered in this work has high level of open and interconnect pores, as shown in Fig. 3. Thus, it is reasonable that the strength data for these foamed ceramics were closer to the open-cell foam model.

However, the lack of good fitting to the Ashby's open-cell model is most likely associated to absence of microstructural parameters for the foamed ceramics, which may involve other properties besides the relative density and type of pores or cells. Colombo et al. [5] also related the lack of fitting of mechanical properties of Silicon Oxycarbide ceramic foams with Ashby's model (Fig. 3) to microstructural factors.

In order to check the validity of Zheng's model, the fracture flexural strength data of foamed Al_2O_3 produced in this work were considered. Nevertheless, the results must be interpreted with caution, as Zheng's model overestimated the flexural strength leading to values close to 25 MPa, whereas the average experimental one was 10 MPa. The problem is challenging because pore features differ depending on the processing. Then, it is not expected that a simple model will exactly represent the behaviour of the actual porous ceramics.

Based on the results attained, this work suggests that a parameter which expresses the processing method to produce the porous structure should also be considered by the mechanical models. Although porous ceramics with similar porosity and density ranges can be produced by different ceramic methods, such as sacrificial fugitives, replica templates and directing foaming [1, 2], each one provides pore walls with distinct solids particles packing, which will influence the final mechanical behavior of material.

It can thus be suggested that the packing coefficient (q) or the average density of the individual struts or, even, the number of connecting struts might represent the missing parameter for a suitable modeling.

Regarding the fracture energies, as well as the fracture toughness values, of foamed Al_2O_3 ceramics they are presented in Tab. 2 and the fracture surface microstructure is shown in Fig. 4.

Tab. 2 Summary of mechanical properties of foamed Al_2O_3 ceramics

Density, ρ [g/cm³]	Flexural Strength σ_f [MPa]	Compressive Strength σ_c [MPa]	E-Modulus [GPa]	Fracture Energy γ_{NBT} [J/m²]	Fracture Toughness K_{IC} [MPa.m$^{1/2}$]	Work of Fracture γ_{WOF} [J/m²]
0,90 ± 0,03	10,32 ± 1,20	20,36 ± 2,50	16,81 ± 1,57	6,82 ± 1,57	0,48 ± 0,05	11,26 ± 2,33

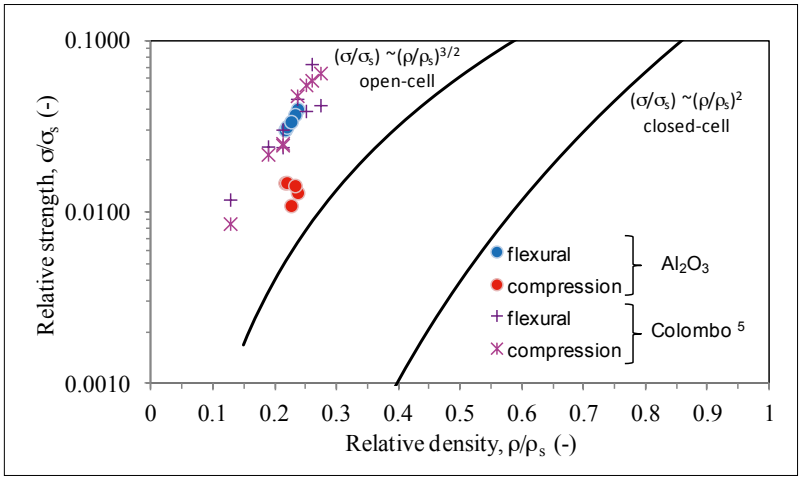

Fig. 3 Data of flexural and compression relative strength as a function of relative density of foamed Al_2O_3. The solid lines correspond to the Ashby and Gibson's [3, 4] models. The reference values in equation (1) for flexural and compression strengths of solid Al_2O_3 were σ_s = 300 MPa and σ_s = 1,5 GPa, respectively

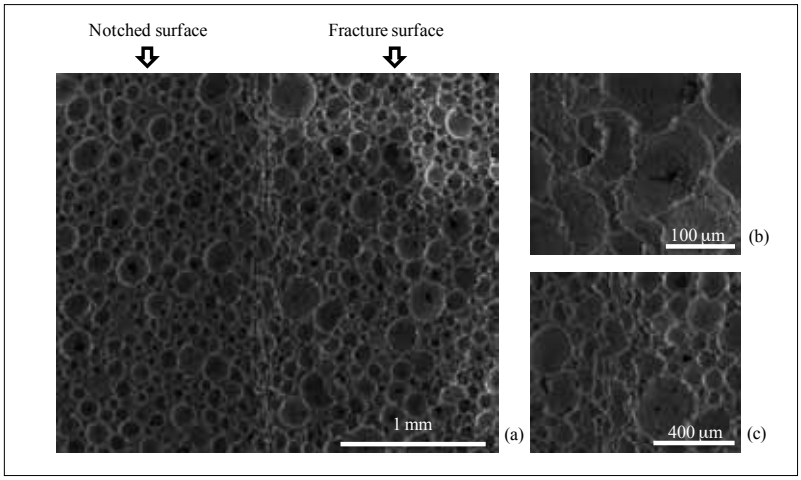

Fig. 4 Fracture surface of foamed Al_2O_3: (a) features of the fracture and notched surfaces, (b) details of pores walls and (c) crack branching in fracture surface

The results of total work-of-fracture energy presented in Tab. 2 agree with those obtained for Al_2O_3 produced with fine grain-size (<20 µm) [13].

Nevertheless, there is a lack in the literature concerning data of fracture energies of foamed ceramics.

The toughness values (K_{IC}) of foamed Al_2O_3 (Tab. 2) are close to those expected for highly porous ceramics. However, these data must be interpreted with reservation, as the stress-intensity factor at the notch tip is most likely lower due to the surrounding pores (Fig. 5). Consequently, the crack propagation should not follow the required linear-elastic conditions for the toughness measurement.

4 Conclusions

This work has shown that the mechanical strength and the Weibull modulus increased when the foaming equipment was used to

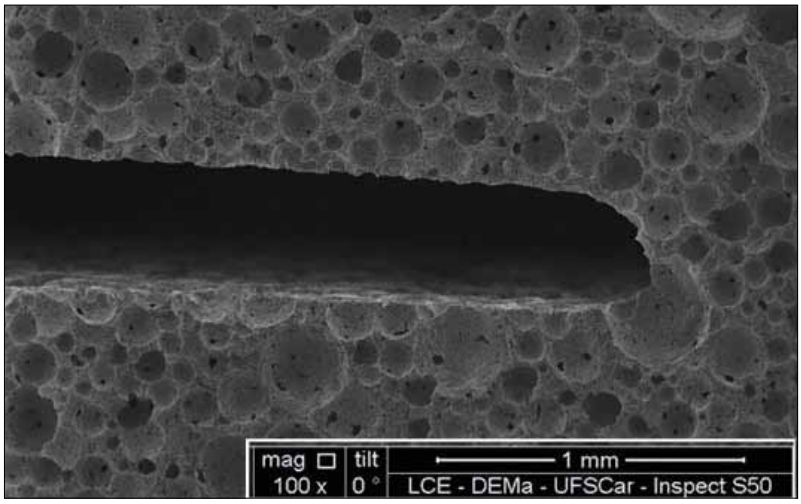

Fig. 5 Surface of foamed Al_2O_3 showing pores at the notch tip

produce macro-porous ceramics of different compositions.

The lack of a good fitting of the strength data of the foamed Al_2O_3 ceramics to Ashby's equation can be related to the need of including microstructural material features in the modeling. This work suggests that a parameter which expresses the foaming processing method should be also considered in mechanical modeling of porous ceramics. The fracture surface analysis points out that the toughness data of Al_2O_3 foam must be interpreted carefully, as the stress-intensity factor at the notch tip may be decreased by the surrounding pores.

Finally, the paper highlights that the understanding processing techniques and the evaluation methods of porous ceramics is the correct path to generate suitable materials that could attain the requirements for a more sustainable environment where saving energy is a key issue.

Acknowledgements

The authors are thankful for the financial support of FIRE, CNPq, UFSCar and USP to carry out this work.

References

[1] Ohji, T.; Fukushima, M.: Macro-porous ceramics: Processing and properties. Int. Mater. Rev. **57** (2012) 115–131

[2] Salvini, V.R.; et al.: Green and reliable macro-porous ceramic processing. Accepted paper for publication in The Amer. Ceram. Soc. Ceramic Transactions from the MS&T13 meeting.

[3] Ashby, M.F.: The mechanical properties of cellular solids. Metall. Trans. A. **14** (1983) 1755–1769

[4] Gibson, L.J.; Ashby, M.F.: Cellular solids, structure and properties. 2nd Ed. Cambridge 1999

[5] Colombo, P.; Hellmann, J.R.; Shelleman, D.L.: Mechanical properties of silicon oxycarbide ceramic foams. J. Amer. Ceram. Soc. **84** (2001) 2245–2251

[6] Rice, R.W.: Relation of tensile strength-porosity effects in ceramics to porosity dependence of Young's modulus and fracture energy, porosity character and grain size. Mater. Sci. and Engin. A112 (1989) 215–224

[7] Zheng, M.; Zheng, X.; Luo, Z.J.: Fracture strength of brittle porous materials. Int. J. of Fracture **58** (1992) R51–R55

[8] Sakai, M.; Ichikawa, H.: Work-of-fracture of brittle materials with microcracking and crack bridging. Int. J. of Fracture **55** (1989) 65–79

[9] Salvini, V.R.; Pandolfelli, V.C.; Bradt, R.C.: Extension of Hasselman's thermal shock theory for crack/microstructure interactions in refractories. Ceramics Int. **38** (2012) 5369–5375

[10] Pickett, G.: Equations for computing elastic constants from flexural and torsional resonant frequencies of vibration of prisms and cylinders. Proc. Amer. Soc. Testing Mater. **45** (1945), 846–865

[11] Kingery, W.D.; Bowen, H.K.; Uhlmann, D.R.: Introduction to ceramics. 2nd Ed. New York 1976, 787–790

[12] Magrabi, S.A.; Dlugogorski, B.Z.; Jameson, G.J.: Bubble size distribution and coarsening of aqueous foams. Chem. Engin. Sci. **54** (1999) 4007–4022

[13] Doerre, E.; Huebner, H.: Alumina: Processing, properties, and applications. Berlin 1984, 81–95